DELPHI Collaboration DELPHI 97-33 PHYS 686
7 April, 1997

Search for SUSY particles mass-degenerate with the LSP at LEP2

S. Paiano, A. Perrotta, T. Rovelli, M. Verardi
INFN and Università - Bologna

Abstract

A search for charginos and neutralinos mass-degenerate with the lightest supersymmetric particle has been carried out at LEP center-of-mass energies between 130 and 172 GeV. The otherwise overwhelming background coming from $\gamma\gamma$ events has been put under control by looking for initial state radiation emitted in the event. In the case of the charginos a detailed study has been performed for degeneracies between 0.5 and 3 GeV. Two regions in the space of the SUSY parameters permit such a degeneracy: while in the low $|\mu|$, large M_2 region the lower cross section does not allow to set limits with the integrated luminosity collected so far, in the high $|\mu|$, low M_2 case charginos with mass below 53.4 GeV/c^2 have been excluded at the 95% CL, provided the sneutrino mass is above 500 GeV/c^2.

1 Introduction

The Standard Model (SM) has received a strong support from the precise results obtained in the phase 1 of LEP, with centre-of-mass energies around the Z^0 pole. No deviation from the SM expectations has been found. However, that model can hardly be extrapolated toward higher energy domains to explain the phenomenology expected at the Planck scale: theorists believe that it is only the low energy approximation of a more general theory in which new particles and some further symmetry requirement solve the high energy problems of the SM.

Amongst the theories having the SM as a low energy approximation, there is particular interest in supersymmetry (SUSY) [1], in which the supposed symmetry between fermions and bosons requires that new (s)particles must exist mirroring the known particles. The non observation of SUSY particles having the same mass as their ordinary matter superpartners means that supersymmmetry is not an exact symmetry, but must be broken somehow at low energies.

In the last two years the LEP centre-of-mass energy ($E_{\rm cms}$) has been brought up to 172 GeV, thus permitting the direct search for all sparticles kinematically admitted in a region of masses which is highly favoured theoretically. Several searches have been already carried out in the DELPHI experiment [2]; since there is no evidence of excesses above the SM expectations, the phase space allowed for the SUSY parameters has been significantly restricted.

The well tested lepton and baryon number conservation in standard physics favours supersymmetric theories in which a quantum number, called R-parity, must be conserved. It follows that sparticles cannot decay into ordinary particles alone: instead, there must exist a lightest supersymmetric particle (LSP) which remains as an ash of any SUSY decay chain. It is a common assumption that the LSP is neutral and only weakly interacting. Then, the final result of an e^+e^- annihilation into a pair of sparticles consists typically in visible ordinary particles plus the missing energy carried away by the two LSP's. The normal way of probing SUSY is therefore to look for particles accompanied by some missing energy. This works while the mass difference between the produced sparticle and the LSP is large enough to leave some reasonable amount of energy to the final state particles. Typically, the searches carried out so far at LEP in the different SUSY channels stopped at mass differences of the order 3-5 GeV/c^2. For example, DELPHI at LEP2 excluded the existence of charginos, neutralinos, sleptons and $\tilde{b}$ and $\tilde{t}$ squarks below their computed upper limit, provided the mass difference between the sparticles searched for and the LSP is above 5 GeV/c^2 [2]. For smaller mass differences, the only limits available so far are those obtained at LEP1, which ruled out charged SUSY particles lighter than about $M_Z/2$ [3].

What is the technical challenge of the low ΔM regions? Let us consider the case of the chargino. If $\Delta M = M(\tilde{\chi}^{\pm}_1) - M(\tilde{\chi}^0_1)$ is lower than m_e, then the chargino has no standard charged particle in which to decay and then it acts exactly as a LSP. If ΔM is only slightly higher than m_e, then the chargino lifetime can still be so long that it passes through the whole detector before decaying. In DELPHI such a region (up to $\Delta M \simeq 100$ MeV/c^2) is covered by looking for heavy charged particles identified with the RICHes and/or releasing an anomalously high ionization in the TPC [4]. The region at slightly higher ΔM has been covered by looking for kinks originating from a chargino decay inside the detector but significantly displaced from the main interaction point [5].

For still larger mass differences the chargino decay length is so short that the chargino decay vertex cannot be distingushed from the production one. However the visible particles carry only a minute fraction of the available energy. Usual cuts against $\gamma\gamma$ events require a minimum visible tranverse momentum (P_T), thus being quite inefficient, if not completely blind, for those final states. On the other hand, it is not possible to remove the P_T cut completely without being flooded with the $\gamma\gamma$ background, which has a cross section orders of magnitude higher than any signal searched for at LEP2.

Here a suggestion initially proposed in [6] is followed to recover those events with highly degenerate sparticles. If one considers only the events accompanied by a hard photon radiated in the initial state (ISR), then the $\gamma\gamma$ background can be kept under control in the following way. If the photon transverse energy is chosen to be greater than

$$(E_\gamma^T)^{\min} = \sqrt{s} \cdot \frac{\sin\theta_{\min}}{1+\sin\theta_{\min}} \quad , \tag{1}$$

where $\theta_{\min}$ is the lowest polar angle accessible in the detector, then typically at least one of the final state electrons, which usually escapes undetected in the beam pipe in a $\gamma\gamma$ event, should be deflected at $\theta_e > \theta_{\min}$, thus allowing the event to be identified and discarded as a background one.

The price to be paid with such a selection is in terms of the efficiencies, because only a few percent of the SUSY events has an ISR photon with $E^T > (E_\gamma^T)^{\min}$, given the $\theta_{\min}$ provided by the inner acceptance of the LEP luminometers. It means that a lot of statistics is needed to get meaningful results: only a limited part of the space of SUSY parameters can be excluded with the present search, waiting for more data from LEP or from the combination with analogous results of the other experiments to explore a wider area. On the other hand, this is so far the only attempt proposed to cover such a degenerate region.

Only degenerate charginos and neutralinos will be considered in the present study, letting aside other sparticles while waiting for an enlarged statistics.

2 Data samples and event generators

A detailed description of the DELPHI detector and its performances can be found in [7]. The integrated luminosities used are respectively 2.9, 3.1, 9.9 and 10.0 pb^{-1} at the centre-of-mass energies of 130, 136, 161 and 172 GeV. Only runs in which the main tracking device and the electromagnetic calorimeters work correctly have been taken into account. The small statistics accumulated at 140 GeV have been merged with those at 136 GeV, and those at 170 GeV have been merged with the one at 172 GeV.

To evaluate the signal efficiency and the background contamination, events were generated using several different programs, all relying on JETSET 7.4 [8] for quark fragmentation. All generated events were passed through a complete simulation of the DELPHI detector [9], and then processed in exactly the same way as the real data.

The program SUSYGEN [10], which includes ISR, was used to simulate chargino and neutralino events. At every centre-of-mass energy, 2000 $e+e- \to \tilde{\chi}_1^+\tilde{\chi}_1^-$ events were generated with chargino masses of 45, 50, 60 and 70 GeV/c^2 (the last point was not kinematically allowed at 130-136 GeV) and mass differences of the order of 0.5, 1 and 3 GeV/c^2. $e^+e^- \to \tilde{\chi}_2^0\tilde{\chi}_1^0$ events were generated at $\sqrt{s} = 161$ GeV, with the same $\tilde{\chi}_2^0$ masses as the chargino ones and mass differences of 1 and 3 GeV/c^2.

For the SM background, several samples of the different final states were generated with statistics which were at least 3-4 times (in the worst cases) those expected. Radiative Z^0 decays ($e^+e^- \to Z^0\gamma$, $Z^0 \to$ anything) and four-fermion processes were generated with PYTHIA [8]. For the $\gamma\gamma$ collisions, the generator of Berends, Daverveldt and Kleiss (BDK) [11] was used for the leptonic final states, where the $(e^+e^-)\mu^+\mu^-$ and $(e^+e^-)\tau^+\tau^-$ final states included the simulation of the transverse energy of the ISR photon, while in $(e^+e^-)e^+e^-$ it was not implemented. In the $\gamma\gamma$ collisions leading to hadronic final states, the QCD and VDM parts were simulated with the TWOGAM [12] generator (which has no transverse energy associated to the ISR photon), while BDK with visible ISR was used for the QPM part. Although not used for the computation of the background, $\gamma\gamma \to$ QPM events were also generated using the TWOGAM generator, in order to study the differences between the two codes, mainly those related to the non-inclusion of ISR photons with visible transverse energy in TWOGAM.

3 Chargino and Neutralino production and decay at low $\Delta(M)$

The Higgsino and gaugino sector of the minimal SUSY can be described in term of four parameters: the ratio $\tan\beta$ of the two Higgs vacuum expectation values, the Higgs mixing parameter μ, the SU_2 gaugino mass M_2 and the U_1 gaugino mass M_1. In most models the gaugino mass unification is foreseen at the GUT scale, which gives a relation between M_1 and M_2

$$M_1 = \frac{5}{3}\tan^2\theta_W \cdot M_2 \simeq 0.5 \cdot M_2 \quad . \tag{2}$$

However, the unification condition above is not strictly necessary in the theory and several models exist without it. In particular, [13] proposes a non-standard string/SUSY scenario which can naturally give rise to a chargino and the second neutralino mass-degenerate with the $\tilde{\chi}^0_1$ (LSP). In the following the definition

$$M_1 = R_f \cdot \frac{5}{3}\tan^2\theta_W \cdot M_2 \tag{3}$$

will be used, so that any value of R_f different from 1 indicates how much the model deviates from the gaugino mass unification hypothesis.

In minimal SUSY there are two charginos ($\tilde{\chi}^\pm_1$ and $\tilde{\chi}^\pm_2$): these mass eigenstates are linear combinations of the two interaction eigenstates, the wino and the charged higgsino. Also four neutralinos exist, linear combinations of the neutral interaction eigenstates. In the following it will be assumed that the lightest neutralino is the LSP.

The lightest chargino is mass-degenerate with the LSP in two cases [6]:

- Low μ, large $M_{1,2}$ scenario: $\tilde{\chi}^0_1$ and $\tilde{\chi}^+_1$ are both higgsino-like and nearly degenerate, with masses $\sim \mu$;
- High μ, low M_2: the $\tilde{\chi}^0_1$ and the $\tilde{\chi}^+_1$ are both gaugino-like and degenerate with masses $\sim M_2$. In this scenario, in order to have $\Delta(M)$ of the order of 1 GeV/c^2 or lower, R_f from eq. (3) must be bigger than or equal to 2.

In the first scenario, the next-to-lightest neutralino is also mass-degenerate with the lightest neutralino, with a mass splitting which is approximately twice the chargino one. The same is true also for the second scenario, but limitately to $R_f = 2$.

3.1 Cross sections

The $e^+e^- \to \tilde{\chi}_1^+\tilde{\chi}_1^-$ and $e^+e^- \to \tilde{\chi}_1^0\tilde{\chi}_2^0$ cross sections at the four centre-of-mass energy are shown in figures 1 and 2, as a function of the $\tilde{\chi}_1^\pm$ and $\tilde{\chi}_2^0$ mass. R_f is set to 1 in the higgsino case and to 2 in the gaugino one; in the first case the cross sections are absolutely stable when varying R_f from 1 to 10, and also in the second case the cross sections do not change by more than 5-6% if R_f spans between 2 and 10. The non-zero widths of the curves in the figures come from a variation of $\tan\beta$ from 1 to 50; from a variation of M_2 and μ over all values that are compatible with the sparticle masses indicated in the figure and mass differences between 0.5 and 3 GeV/c^2. The exchange of sfermions in the t-channel interferes destructively with the s-channel exchange, lowering the gaugino cross section at small values of $m_{\tilde{\nu}}$ (for the chargino) and $m_{\tilde{e}}$ (for the neutralino production); in the figures, the sneutrino mass has been varied from M_χ to 1 TeV/c^2 in the higgsino plots, and from 500 GeV/c^2 to 1 TeV/c^2 in the gaugino ones.

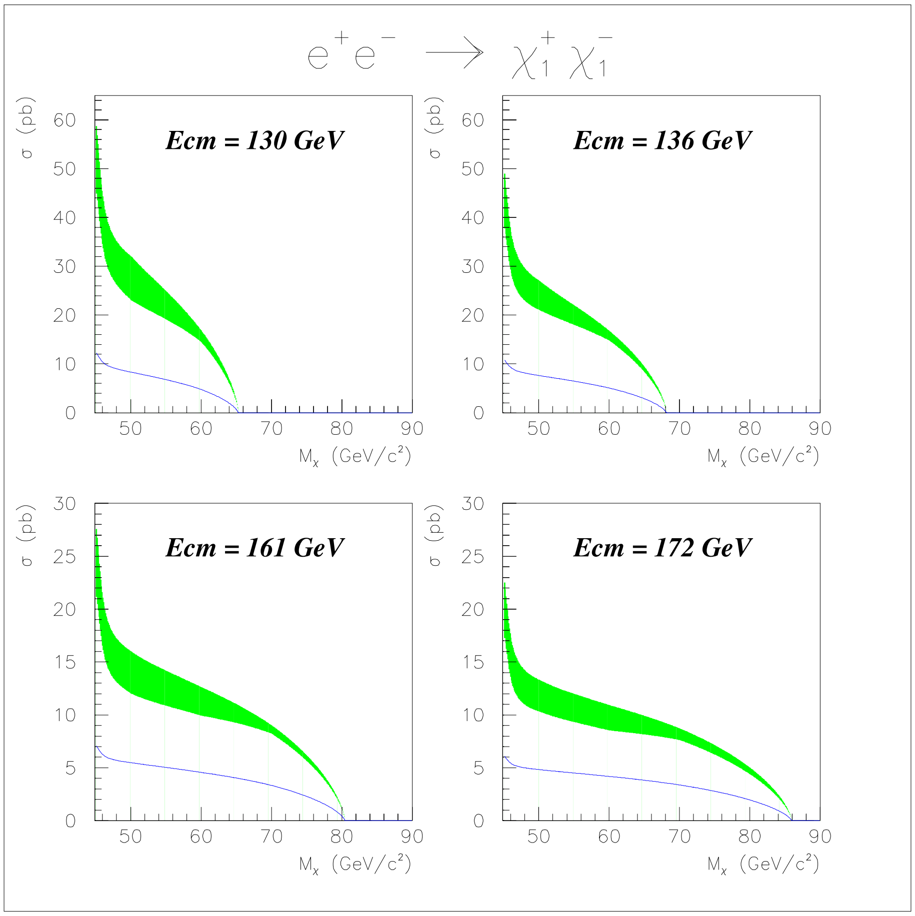

Figure 1: $e^+e^- \to \tilde{\chi}_1^+\tilde{\chi}_1^-$ *cross sections at the four centre-of-mass energies and as a function of the chargino mass. The upper bands refer to the* $M_2 \ll |\mu|$ *gaugino-like scenario; the lower bands to the* $|\mu| \ll M_2$ *higgsino-like one. The widths of the two bands allow for a variation of* M_2 *and* μ *inside the two scenarios so that* $0.5 < \Delta(M) < 3$ GeV/c^2; $1 < \tan\beta < 50$; $M(\tilde{\nu}) > 500$ GeV/c^2 *(gaugino) or* $M(\tilde{\nu}) > M(\tilde{\chi}_1^+)$ *(higgsino).*

For the neutralinos, the $e^+e^- \to \tilde{\chi}_1^0\tilde{\chi}_1^0$ and $e^+e^- \to \tilde{\chi}_2^0\tilde{\chi}_2^0$ cross sections have been found to be much smaller than the $e^+e^- \to \tilde{\chi}_1^0\tilde{\chi}_2^0$ one, shown in the plots. This last will

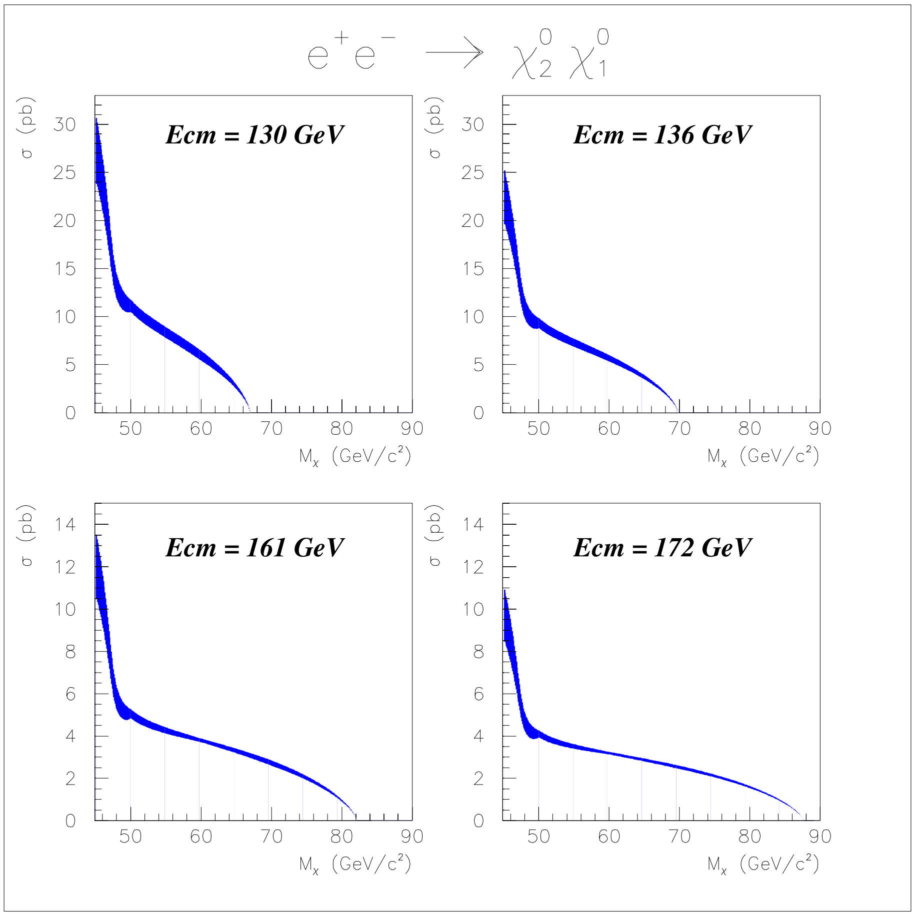

Figure 2: $e^+e^- \to \tilde{\chi}_1^0\tilde{\chi}_2^0$ *cross sections at the four centre-of-mass energies and as a function of the* $\tilde{\chi}_2^0$ *mass. Only the higgsino-like scenario* ($|\mu| \ll M_2$) *is shown, because the gaugino cross sections are in the order of fb. The widths of the bands allow for a variation of* M_2 *and* μ *so that* $0.5 < \Delta(M) < 3$ *GeV/*c^2*;* $1 < \tan\beta < 50$*;* $1 < R_f < 10$*;* $M(\tilde{e}) > M(\tilde{\chi}_2^0)$.

be the only process e^+e^- going to a pair of neutralinos considered in the following.

One can notice that the chargino cross-sections is approximately three times bigger in the gaugino-like scenarios than in the higgsino-like ones. On the contrary, the $\tilde{\chi}_1^0\tilde{\chi}_2^0$ cross section in the gaugino-like scenario is more than three orders of magnitude lower than in the higgsino one.

3.2 Branching ratios

Since the number of signal events potentially visible in the data depends both on the cross section and on the efficiency of the selection criteria, the *inos* decay modes can be quite important for the analysis. The chargino branching ratios have been studied by using two different programs. One is SUSYGEN [10], the standard MonteCarlo used to simulate all SUSY samples in DELPHI. The other is an analytical calculation [13], that will be called CDG for simplicity, in which only the W exchange is implemented; on the other hand, for the low $\Delta(M)$ region the pion resonances form factors are taken into account and it has been checked that the CDG program reproduces the τ decays correctly ($\Delta(M) = m_\tau$). Other relevant differences between the two programs reside in how the masses of the hadronic decay products are inserted and how some approximation has been introduced in SUSYGEN in order to speed up the computation time.

To compare the two programs, the $\tilde{\nu}$ mass has been set to 1 TeV/c^2, thus cancelling any relevant effect of the sfermion exchange in SUSYGEN. The chargino branching ratios depend only on $\Delta(M)$ and not on the particular scenario.

Figure 3 compares the results of the two programs for the branching ratios

$$\tilde{\chi}_1^+ \rightarrow \tilde{\chi}_1^0 e^+ \nu_e \quad (4)$$
$$\tilde{\chi}_1^+ \rightarrow \tilde{\chi}_1^0 \mu^+ \nu_\mu \quad (5)$$
$$\tilde{\chi}_1^+ \rightarrow \tilde{\chi}_1^0 \tau^+ \nu_\tau \quad (6)$$
$$\tilde{\chi}_1^+ \rightarrow \tilde{\chi}_1^0 q \bar{q}' \quad (7)$$

as a function of $\Delta(M)$ for mass differences between 200 MeV/c^2 and 4 GeV/c^2; at still larger $\Delta(M)$ the two programs agree, since the only differences are at low momentum transfer between the $\tilde{\chi}_1^+$ and its ordinary decay products.

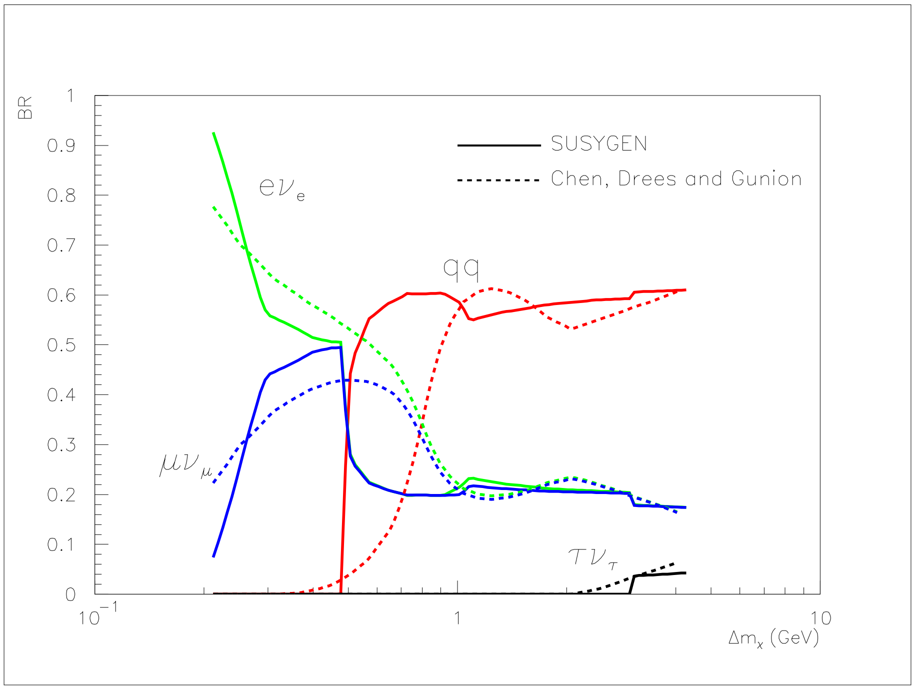

Figure 3: *Branching ratios of the chargino decaying into the LSP plus standard particles, when the mass difference between the chargino and the LSP is below 4 GeV/c^2. The sneutrino mass has been set to 1 TeV/c^2, so that only the s-channel is involved. The outputs of the SUSYGEN (full line) and CDG (dashed line) programs are compared as a function of $\Delta(M)$.*

It is clear that the two programs disagree on all the branchings at low $\Delta(M)$. After removing the low momentum transfer approximations in the SUSYGEN integration routine and adding the mass term in its formulae, then the leptonic decay rates in SUSYGEN and in CDG agree perfectly, as they should[1]. Nevertheless, the hadronic one still does not, because it is computed in a completely different way in the two codes.

[1]The new version 2.0 of SUSYGEN includes these two corrections and has a perfect agreement with the CDG leptonic widths in the degenerate scenario

As observed before, CDG itself has many other limitations that prevent its use as an MC generator spanning the whole phase space. The conclusion of this comparison is that a correct generator for degenerate particles is not yet available, as far as BR's are concerned. In any search for sparticles having a mass-difference with their daughters below 3-4 GeV/c^2, one should quote separately the results for any of the exclusive decay channels or, alternatively, one should use flavour independent selection criteria, so that the final results do not depend on the exclusive decay rates. What has been discussed here for the chargino also holds, qualitatively, for the $\tilde{\chi}^0_2 \to \tilde{\chi}^0_1 X$ decay modes.

It has been found in the present work that the efficiencies of the selection criteria for the degenerate chargino pair production, which will be detailed below, are completely independent from the exclusive decay products. The reason is simple. In the range of $\Delta(M)$ taken into account in the present study, the hadronic decay (7) ends up with almost 100% probability in a final state $\tilde{\chi}^0_1 \pi^+ \pi^0$. Thus all modes (4), (5) and (7) end up in final states with only one charged and one neutral particle, besides the LSP. In (6) there are three neutrals, but this mode is kinematically disfavoured in the degenerate scenario. Since the selection criteria chosen here depend almost completely on the properties of the two remaining charged particles (and on the ISR photon, of course), it is not a big surprise that events with π^+ show the same efficiency as events with e^+ or μ^+.

The same flavour independence of the selection criteria is not valid any more for the $\tilde{\chi}^0_2$ decays. In figure 4 are plotted the exclusive branching ratios of the $\tilde{\chi}^0_2$ as computed with SUSYGEN. Several modes are allowed:

$$\tilde{\chi}^0_2 \to \tilde{\chi}^0_1 \gamma \quad (8)$$
$$\tilde{\chi}^0_2 \to \tilde{\chi}^0_1 l^+ l^- \quad (9)$$
$$\tilde{\chi}^0_2 \to \tilde{\chi}^0_1 q\bar{q} \quad (10)$$
$$\tilde{\chi}^0_2 \to \tilde{\chi}^0_1 \nu\bar{\nu} \quad (11)$$
$$\tilde{\chi}^0_2 \to \tilde{\chi}^+_1 l^- \bar{\nu} \quad (12)$$
$$\tilde{\chi}^0_2 \to \tilde{\chi}^+_1 q\bar{q}' \quad (13)$$

In the gaugino-like scenario, where the $e^+e^- \to \tilde{\chi}^0_2\tilde{\chi}^0_1$ cross section is negligible with respect to the $\tilde{\chi}^+_1\tilde{\chi}^-_1$ one, the decay modes (12) and (13) are dominant.

In the higgsino scenario, where the production cross section is approximately the same as the chargino one, the radiative decay (8) rate increases together with the degeneracy. In the region of interest for the present study, a relevant fraction of the $\tilde{\chi}^0_2$ ends up in a photon or in a pair of neutrinos, besides the LSP. It is hard to unambiguously detect a photon of about 1 GeV in the detector and separate it from the background; thus, in the higgsino scenario a relevant fraction of the $\tilde{\chi}^0_2$ ends up in an absolutely or practically invisible final state.

This is the reason why in both scenarios the present work has been limited to the search for degenerate charginos, letting neutralinos (and other sparticles) aside for the moment.

4 Event selection

The criteria used to select events were defined on the basis of the simulated signal and background events. Charged particles were required to have a momentum above 100

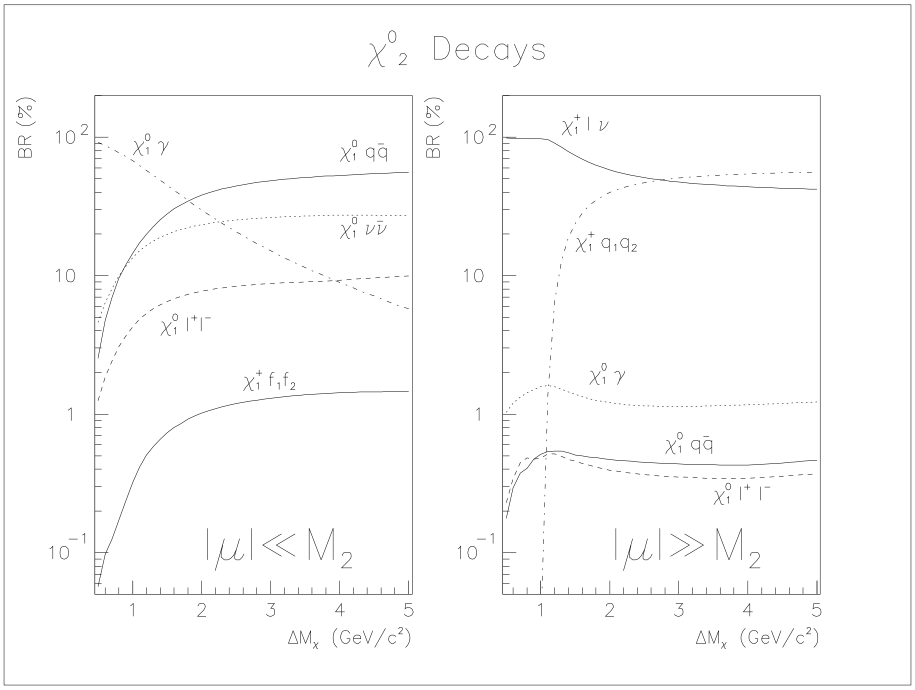

Figure 4: *Branching ratios of the decay modes of the second neutralino decaying into the LSP plus standard particles, when the mass difference between the $\tilde{\chi}_2^0$ and the LSP is below 4 GeV, according to the program SUSYGEN. The left plot referes to the higgsino-like scenario, while on the right are shown the branchings in the gaugino-like scenario.*

MeV/c, known with an error below 100%, impact parameters below 4 cm in $r\phi$ and below 10 cm in z and a track length of at least 30 cm. To reduce the incidence of beam-gas or other spurious events, a primary vertex compatible with the beam spot had to be reconstructed by using at least two of the charged particles.

Neutrals had to have an energy of at least 500 MeV. Both calorimetric deposits and clear photon conversions, as reconstructed by the ELEPHANT package [14], were considered. To reduce the amount of spurious showers in the calorimeters faking a neutral particle in the event, the following criteria have been used. In the HPC at least three of the nine layers must be hit; the first layer hit by the shower must be before the $6^{\rm th}$ HPC layer; not more than 90% of the total energy of the shower can be deposited in a single layer; the θ angle recostructed in the calorimeter must point to the main event vertex within 15^o. In the FEMC the shower must hit at least two towers. In the STIC an energy of more than 2 GeV must be associated to the shower and at least two towers must be hit.

All neutral showers inside a cone with half opening angle of 5^o are recombined together. If, after the recombination, the resulting neutral gets a fraction of hadronic energy above 10% of its total energy it will not be considered as an isolated ISR photon candidate.

All particles not having associated hits in any of the tracking devices of DELPHI have been taken as neutrals. Given the lower reconstruction and association efficiency of tracks in the two endcaps of DELPHI with respect to the barrel, tag electrons from $\gamma\gamma$ events can be seen as calorimetric deposits without the corresponding track elements: if that electron is isolated, it can fake an ISR photon, and special care must be paid to discard those events. In the following, 'photon candidate' will mean a particle without track elements attached to it, not necessarily a 'real photon'.

4.1 Preselection

All the selection cuts are applied on a preselected sample containing events with at least two charged tracks; an isolated (more than 15^o from any other charged or neutral particle in the event) photon candidate of at least 4 GeV, having a transverse energy above 2 GeV and a mass recoiling against the photon of at least 88 GeV/c^2; the visible energy of all particles but the photon representing no more than 10% of the available centre-of-mass energy; no more than 99% of the whole visible energy must be in a single hemisphere inside a cone of half opening angle 60^o. The mass recoiling against the photon is defined as

$$M_{\text{opp}}^2 = E_{\text{cms}}^2 - 2E_{\text{cms}}E_\gamma \tag{14}$$

and requiring M_{opp} to be above a certain value is practically an upper limit on the photon energy.

Notice that all the selection cuts described below consist in some tightening of these preselection cuts. The final selection can be described by adding only the requirement of having at least two charged particles to the cuts described in the next paragraph.

4.2 Selection

Further selection criteria have been applied on the preselected events. They are intended to keep the expected background not above 1 event at each point, while keeping the signal efficiency as high as possible, compatibly with the expected low rate of ISR.

- The main cut against the $\gamma\gamma$ background is the one on the transverse photon energy, E_T^γ. The cut has been defined by inserting in equation (1) the minimum angle visible in the STIC, which is approximately $1.95°$; this automatically defines a cut on the transverse photon energy at any of the centre-of-mass energies taken into account, as can be seen in table 1.

- The mass recoiling against the photon (M_{opp}) must be above 96 GeV/c^2, and according to equation (14) this cut translates into a different upper limit on the photon energy at each E_{cms}; this upper limit is also reported in table 1. Beside the $\gamma\gamma$, this cut is also intended to reduce the rate of radiative Z^0 returns in the final sample.

- The photon is required to be isolated by at least 30^o with respect to any other charged or neutral particle in the event.

- The visible energy of the event, excluding the photon, must be below 5% of E_{cms}.

- The fraction of visible energy inside a double cone of 30^o (E_{30}/E_{vis}) or a single hemisphere cone of 60^o ($E_{\text{Frw}}/E_{\text{vis}}$) both centred on the beam axis must be below, respectively, 60% and 80%. If the photon is inside the cone, its energy is subtracted both from the numerator and from the denominator defining those fractions.

- If there are more than two particles besides the photon in the event, their aplanarity must be above 0.005. The aplanarity is defined as the lowest eigenvalue of the tensor of inertia, provided the three eigenvalues are normalized so that their quadratic sum is equal to 1.

- If the ISR photon candidate is in the STIC region, it must not be correlated with a signal 20 ADC counts above pedestal plus 3σ in any of the two planes of scintillators placed in front of the STIC and acting as Veto Counters [15].

$\sqrt{s}$ (GeV)	$(E_\gamma^T)^{\rm min}$ (GeV)	$E_\gamma^{\rm max}$ (GeV)
130	4.00	29.55
136	4.19	34.12
161	4.96	51.88
172	5.30	59.21

Table 1: *Cut on the minimum transverse energy and on the maximum total energy of the photon candidate as a function of the centre-of-mass energy, according to the explicit formulae given in the text.*

The Veto Counter is not included in the standard DELPHI detector simulation; that's why the corresponding cut has been left as the last one. In the data one looks at the ADC content of the scintillators in the two planes, while in the MC one estimates the number of events passing that cut with the help of the known efficiencies of that detector: using radiative bhabhas and $e+e- \to Z^0\gamma$ events it has been estimated that almost all electrons ($\simeq 99\%$) are killed while approximately 60% of the photons survive that cut.

Figure 5 shows the comparison of the distributions of the above variables between data and the sum of all SM expectations for the 161 GeV preselected samples. The agreement is quite reasonable in almost all distributions. The discrepancy in the last bin of the $M_{\rm opp}$ plot consists of low energy photons which will be discarded during the selection. The discrepancy in the first bin of the plot showing the fraction of energy at low angles is a bit more tricky: in fact in the data there are more events with all particles at large polar angles with respect to the background MC. This discrepancy has been studied. By comparing the two MC of $\gamma\gamma \to$ QPM (BDK, with the simulation of the ISR with transverse energy, and TWOGAM, which does not allow such an ISR photon with transverse energy) it has been verified that, qualitatively, the inclusion of the visible ISR can enhance the number of events with all the particles (but the 'photon candidate') emitted at large angle, that is the first bin of the plot. Since three of the $\gamma\gamma$ final states taken into account have not been simulated with visible ISR photons (e^+e^-, VDM and QCD, the last two representing alone the biggest part of the events remaining after the preselection) this could explain the discrepancy. Moreover, once the cut on E_γ^T, which is the main cut against $\gamma\gamma$, is applied such a discrepancy disappears; it will not be taken into account any more when estimating the overall background level.

The data-MC comparison on the preselected samples at 172 GeV reported in figure 6 looks a bit worse: beside the excess in the first bin of the plot showing the fraction of

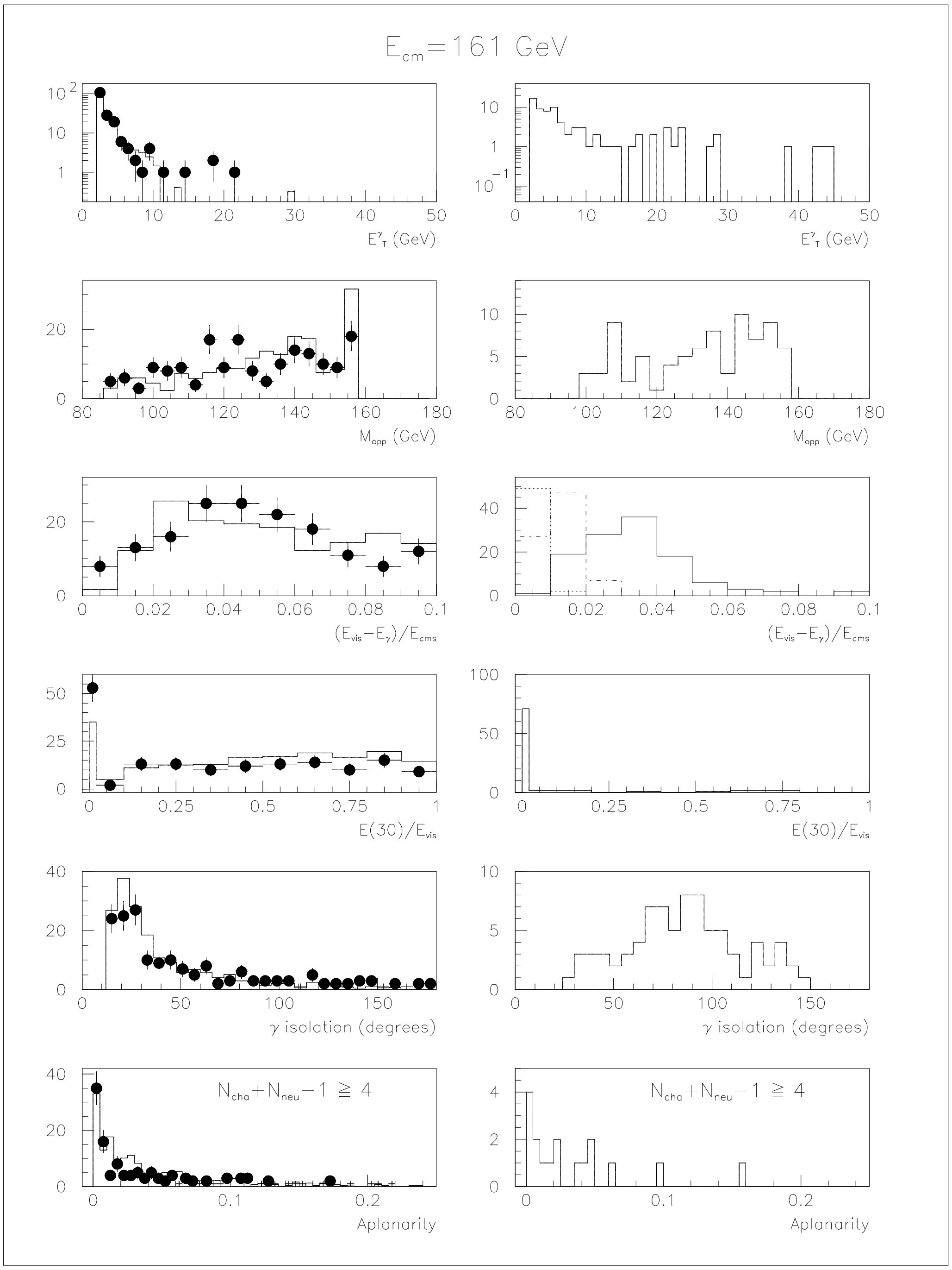

Figure 5: *Some of the variables used in the selection at 161 GeV. In the left plots the data (dots) are compared with the SM expectations. On the right, as an example, the corresponding distributions (with arbitrary normalization) are shown for the signal of mass 50 GeV/c^2 and $\Delta(M)$ = 1 GeV/c^2. In the plot of the visible energy all the three degeneracies are shown for M_χ = 50 GeV/c^2: dotted, $\Delta(M)$ = 0.5 GeV/c^2; dashed, $\Delta(M)$ = 1 GeV/c^2; full line, $\Delta(M)$ = 3 GeV/c^2. In the plot of the aplanarity enter only events with more than three visible particles.*

energy at low angles, there is also a clear excess of events at small aplanarity (but only events with more than three visible particles enter this plot, ie only a small fraction of the whole signal sample). However, this excess is in a region discarded by the selection cuts: a satisfactory agreement is restored after the cuts on the photon energy and on aplanarity. Thus, at 172 GeV too, the estimate of the background remaining after applying all the selection cuts is considered reliable.

As a comparison, in both the figures referring to 161 and 172 GeV are also shown, with arbitrary normalization, the corresponding distributions for charginos of mass 50 GeV/c^2 and degenerate with the lowest neutralino (LSP) of 0.5, 1 and 3 GeV/c^2.

No detailed study of the background has been done for the points at 130 and 136 GeV. The luminosity collected there represents only a small fraction of the whole and, a posteriori, since no candidates have been found at those energies, there is no need to have a precise evaluation of the background content there to set the limits.

All these cuts have been defined by comparing signal and background MC's at 161 GeV; the rescaling with the centre-of-mass energy is implicitly included in the definitions chosen.

5 Results

In table 2 one can see the effect of the cuts on data and standard MC at the two centre-of-mass energies of 161 and 172 GeV; the discrepancies appearing after the first cuts at 172 GeV have already been discussed in the last section. Only data are shown for the two energies of 130 and 136 GeV. No candidates remain at 130, 136 and 161 GeV while at 172 GeV one event survives all cuts. The expected background in the last two points is respectively 0.82 and 0.92 events.

The selection efficiency for degenerate charginos at all centre-of-mass energies is reported in table 3. It must be stressed that the very low signal efficiency comes from the necessary requirement of having a hard ISR photon radiated at visible angles: when the chargino mass increases, the ISR photon becomes softer, thus lowering the overall event selection efficiency. Since this efficiency have been checked to be the same independently of the final state in the chargino decay, the following results do not depend on the specific assumptions about the particular chargino decay mode.

The trigger efficiency in DELPHI is practically 100% for most of the accessible final states. However, in the present search one looks for few particles of very low momentum, accompanied by an energetic photon. Below transverse momenta of the order of 1-2 GeV/c the single track trigger efficiency starts to decrease [16]. That's why for the present analysis a dedicated and detailed study of the trigger performances at low visible and trasverse energy has been carried out. The trigger efficiencies for events having a visible and transverse energy similar to the one of the system accompanying the ISR photon in the signal samples which pass the selection cuts have been computed from the data themselves. All events triggered by the STIC luminometer represent the sample from which to compute the trigger efficiency for the 'large angle' part of the events, since the STIC and the other triggers can be completely decorrelated. As an example, figure 7 shows the trigger efficiency in DELPHI for all energies above the Z^0 as a function of the total transverse energy of the event. The same bins in $E_T^{\rm vis}$ have been used to weight the selected signal events with their 'non-photonic' component of the trigger efficiency. The

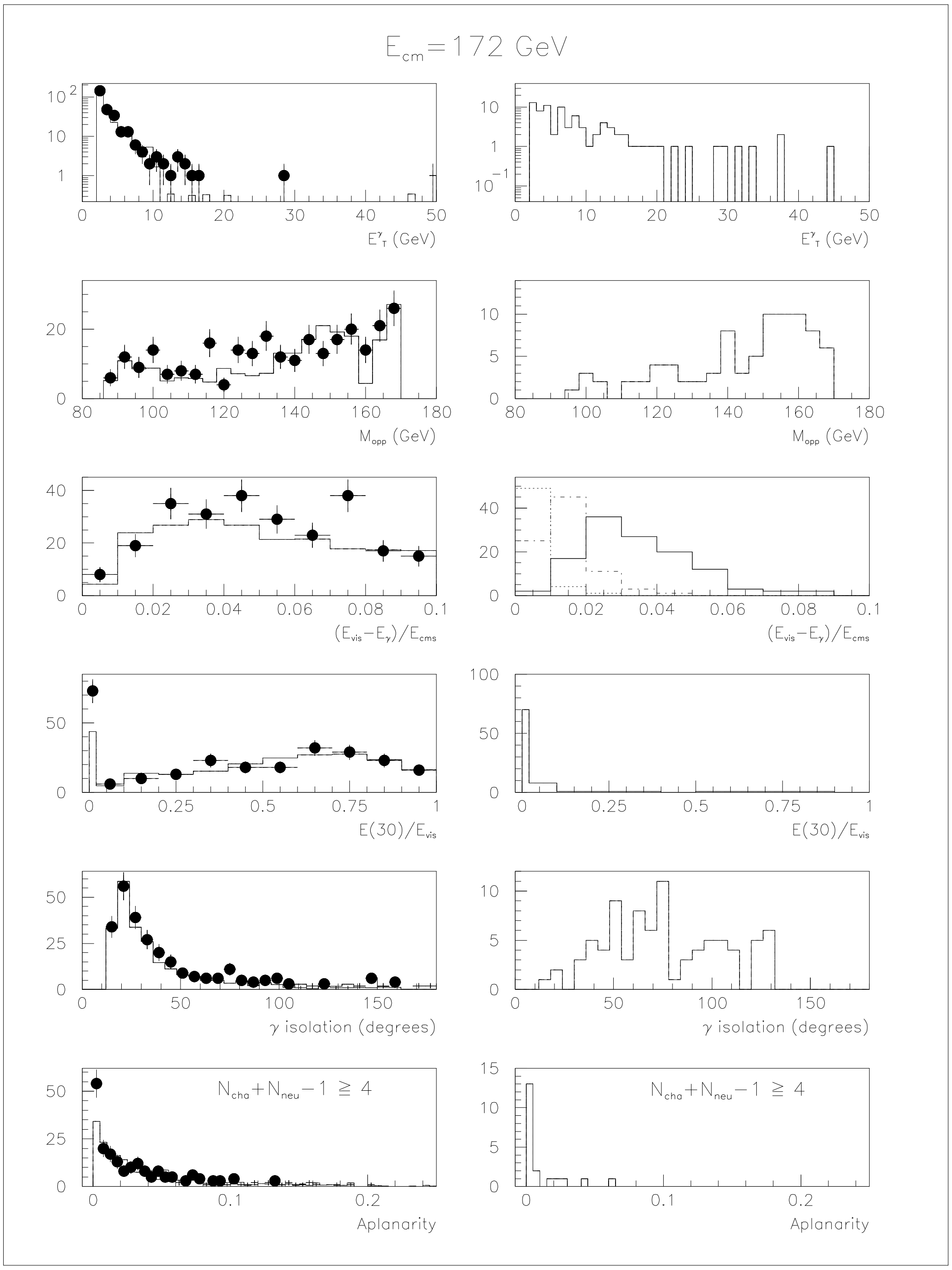

Figure 6: *Same as figure 5, but data and simulation refer to the samples at 172 GeV.*

	E_γ^T,$M_{\rm opp}$	γ isol.	$E_{\rm vis}$	low angles	Aplan.	STIC veto
$E_{\rm cms} = 130/136$ GeV						
Data	13	7	2	1	0	0
$E_{\rm cms} = 161$ GeV						
$\gamma\gamma \to e^+e^-$	0.80	0.80	0.	0.	0.	0.
$\gamma\gamma \to \mu^+\mu^-$	0.47	0.47	0.	0.	0.	0.
$\gamma\gamma \to \tau^+\tau^-$	3.57	2.52	1.22	0.96	0.35	$0.17^{+0.11}_{-0.09}$
$\gamma\gamma \to$ VDM	4.23	2.28	0.65	0.65	0.65	$0.65^{+0.65}_{-0.33}$
$\gamma\gamma \to$ QPM	5.12	2.76	0.79	0.79	0.39	0.
$\gamma\gamma \to$ QCD	2.91	1.66	0.	0.	0.	0.
$e^+e^- \to Z^0\gamma$	0.75	0.45	0.10	0.05	0.	0.
Σ backgrounds	17.85	10.94	2.76	2.45	1.39	$0.82^{+0.66}_{-0.34}$
Data	18	9	2	1	0	0
$E_{\rm cms} = 172$ GeV						
$\gamma\gamma \to e^+e^-$	1.45	0.73	0.	0.	0.	0.
$\gamma\gamma \to \mu^+\mu^-$	1.78	1.19	0.30	0.30	0.30	0.
$\gamma\gamma \to \tau^+\tau^-$	3.14	2.09	0.89	0.72	0.56	$0.16^{+0.16}_{-0.08}$
$\gamma\gamma \to$ VDM	5.14	2.74	0.68	0.68	0.68	$0.68^{+.68}_{-0.34}$
$\gamma\gamma \to$ QPM	8.69	5.21	0.70	0.70	0.70	0.
$\gamma\gamma \to$ QCD	6.66	1.27	0.	0.	0.	0.
$e^+e^- \to Z^0\gamma$	1.05	0.62	0.08	0.08	0.04	$0.04^{+.04}_{-0.03}$
$e^+e^- \to W^+W^-$	0.02	0.01	0.	0.	0.	0.
$e^+e^- \to Z^0e^+e^-$	0.11	0.09	0.05	0.05	0.04	$0.04^{+.04}_{-0.02}$
Σ backgrounds	28.04	13.95	2.70	2.53	2.32	$0.92^{+.70}_{-0.35}$
Data	38	24	4	3	2	1

Table 2: *Effect of the selection cuts on the data and on the expected SM background in the four sets of data taken into account. For* 130 *and* 136 *GeV no detailed study of the background has been done, see text.*

	$M_\chi = 45$	$M_\chi = 50$	$M_\chi = 60$	$M_\chi = 70$
$E_{\rm cms} = 130$ GeV				
$\Delta(M) = 0.5$	$(1.1 \pm 0.2)\%$	$(0.8 \pm 0.2)\%$	$(0.2 \pm 0.1)\%$	-
$\Delta(M) = 1.0$	$(1.4 \pm 0.3)\%$	$(0.9 \pm 0.2)\%$	$(0.2 \pm 0.1)\%$	-
$\Delta(M) = 3.0$	$(1.3 \pm 0.3)\%$	$(1.0 \pm 0.2)\%$	$(0.2 \pm 0.1)\%$	-
$E_{\rm cms} = 136$ GeV				
$\Delta(M) = 0.5$	$(1.0 \pm 0.2)\%$	$(1.1 \pm 0.2)\%$	$(0.3 \pm 0.1)\%$	-
$\Delta(M) = 1.0$	$(2.0 \pm 0.3)\%$	$(1.1 \pm 0.2)\%$	$(0.2 \pm 0.1)\%$	-
$\Delta(M) = 3.0$	$(1.5 \pm 0.3)\%$	$(1.3 \pm 0.3)\%$	$(0.5 \pm 0.2)\%$	-
$E_{\rm cms} = 161$ GeV				
$\Delta(M) = 0.5$	$(1.5 \pm 0.3)\%$	$(1.1 \pm 0.2)\%$	$(1.0 \pm 0.2)\%$	$(0.3 \pm 0.1)\%$
$\Delta(M) = 1.0$	$(2.7 \pm 0.4)\%$	$(2.2 \pm 0.3)\%$	$(1.1 \pm 0.2)\%$	$(0.6 \pm 0.2)\%$
$\Delta(M) = 3.0$	$(1.9 \pm 0.3)\%$	$(2.0 \pm 0.3)\%$	$(1.4 \pm 0.3)\%$	$(0.7 \pm 0.2)\%$
$E_{\rm cms} = 172$ GeV				
$\Delta(M) = 0.5$	$(1.2 \pm 0.2)\%$	$(1.3 \pm 0.2)\%$	$(1.0 \pm 0.2)\%$	$(0.3 \pm 0.1)\%$
$\Delta(M) = 1.0$	$(1.6 \pm 0.3)\%$	$(1.9 \pm 0.3)\%$	$(1.3 \pm 0.3)\%$	$(0.8 \pm 0.2)\%$
$\Delta(M) = 3.0$	$(1.6 \pm 0.3)\%$	$(1.8 \pm 0.3)\%$	$(1.3 \pm 0.3)\%$	$(0.7 \pm 0.2)\%$

Table 3: *Selection efficiency for the chargino signal, computed at the different centre-of-mass energies as function of the chargino mass and of the degeneracy.*

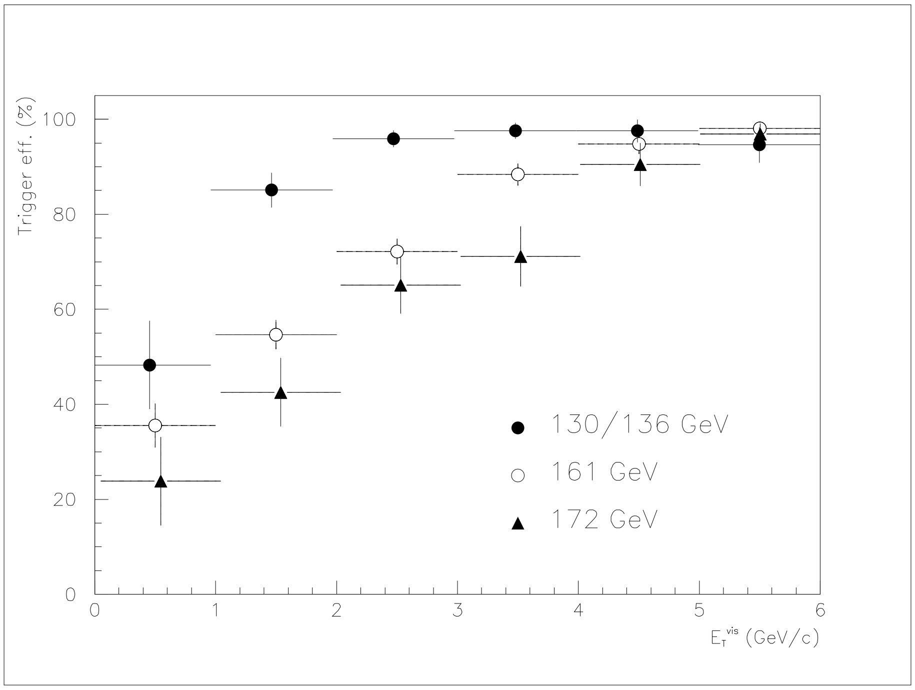

Figure 7: *Trigger efficiency in DELPHI for events at low total visible energies, for data taken during the three runs of LEP above the Z^0 mass, as a function of the transverse energy of the event. The worse performances in the runs at higher energy is due to the necessary downscaling of the $\gamma\gamma$ trigger components during those runs.*

overall trigger efficiency for the signal is then estimated as the logical OR of the known single photon trigger efficiency [17] and the low momentum trigger efficiency previously computed. Such an estimate could be somewhat conservative, because the coincidence of the photon and some of the remaining signals can, sometimes, generate a further independent trigger signal.

Moving from $E_{\rm cms} = 130/136$ GeV to $E_{\rm cms} = 161$ or 172 GeV, the $\gamma\gamma$ cross section goes up; at the same time, but independently, also the noise from the LEP machine increased. This caused an higher rate of the low P^T triggers. To keep the acquisition dead time at a reasonable level, those low P^T trigger components had to be progressively scaled down: this resulted in a reduced 'non-photonic' trigger efficiency for the signal in the last two sets of data (see again figure 7). Also the STIC single γ trigger had to be downscaled during some of the 172 GeV runs, but given the E^T_γ cut this did not affect so much the overall trigger efficiency. In table 4 are reported the trigger efficiencies estimated at the different centre-of-mass energies as a function of $M(\chi)$ and $\Delta(M)$.

A graphical view of the candidate remaining at 172 GeV is shown in figure 8. It consists of a 7.9 GeV photon in the HPC and two very acollinear and acoplanar charged tracks, whose calorimetric deposits are inconsistent with coming from an electron whilst the absence of hits in the muon chambers suggests that they are not muons either. There is some activity in the STIC and a deposit of 33.6 GeV in the Very Small Angle Tagger (VSAT), not visible in the figure. The VSAT does not enter in the definition of the quantities used in the selection. This event is therefore perfectly consistent with being a $\gamma\gamma$ with an hadronic final state. It has a visible energy, besides the photon, of $0.027 \cdot E_{\rm cms}$: this value is inconsistent with all signal events having a mass difference of 500 MeV/c^2,

	$M_\chi = 45$	$M_\chi = 50$	$M_\chi = 60$	$M_\chi = 70$
$E_{\rm cms} = 130/136$ GeV				
$\Delta(M) = 0.5$	90.3%	88.9%	85.3%	-
$\Delta(M) = 1.0$	94.9%	95.0%	92.6%	-
$\Delta(M) = 3.0$	98.8%	99.2%	98.3%	-
$E_{\rm cms} = 161$ GeV				
$\Delta(M) = 0.5$	88.5%	87.1%	85.4%	82.3%
$\Delta(M) = 1.0$	91.6%	90.7%	89.9%	86.0%
$\Delta(M) = 3.0$	97.3%	96.7%	95.5%	95.5%
$E_{\rm cms} = 172$ GeV				
$\Delta(M) = 0.5$	87.0%	85.8%	83.5%	80.9%
$\Delta(M) = 1.0$	90.9%	89.0%	88.6%	84.2%
$\Delta(M) = 3.0$	95.8%	95.8%	93.8%	91.9%

Table 4: *Trigger efficiency for the chargino signal, computed at the different center-of-mass energies as function of the chargino mass and of the degeneracy. The relative errors (not shown) are well below the selection efficiency ones and will not be considered when computing the upper limits on the chargino mass.*

is consistent with $\Delta(M) = 3$ GeV/c^2 signal and only marginally consistent with the $\Delta(M) = 1$ GeV/c^2 one. In the calculation of the exclusion limits it will be considered as a candidate only for the charginos with a mass difference of 1 and 3 GeV/c^2.

6 Exclusion limits

Since there is no evidence for a signal at any of the centre-of-mass energies studied, one can derive limits on the production of pairs of charginos mass-degenerate with the LSP.

6.1 Method

Although the cross section is relatively high for all chargino masses (see figure 1), because of the low signal efficiency it is mandatory to combine the data taken at all energies. An-

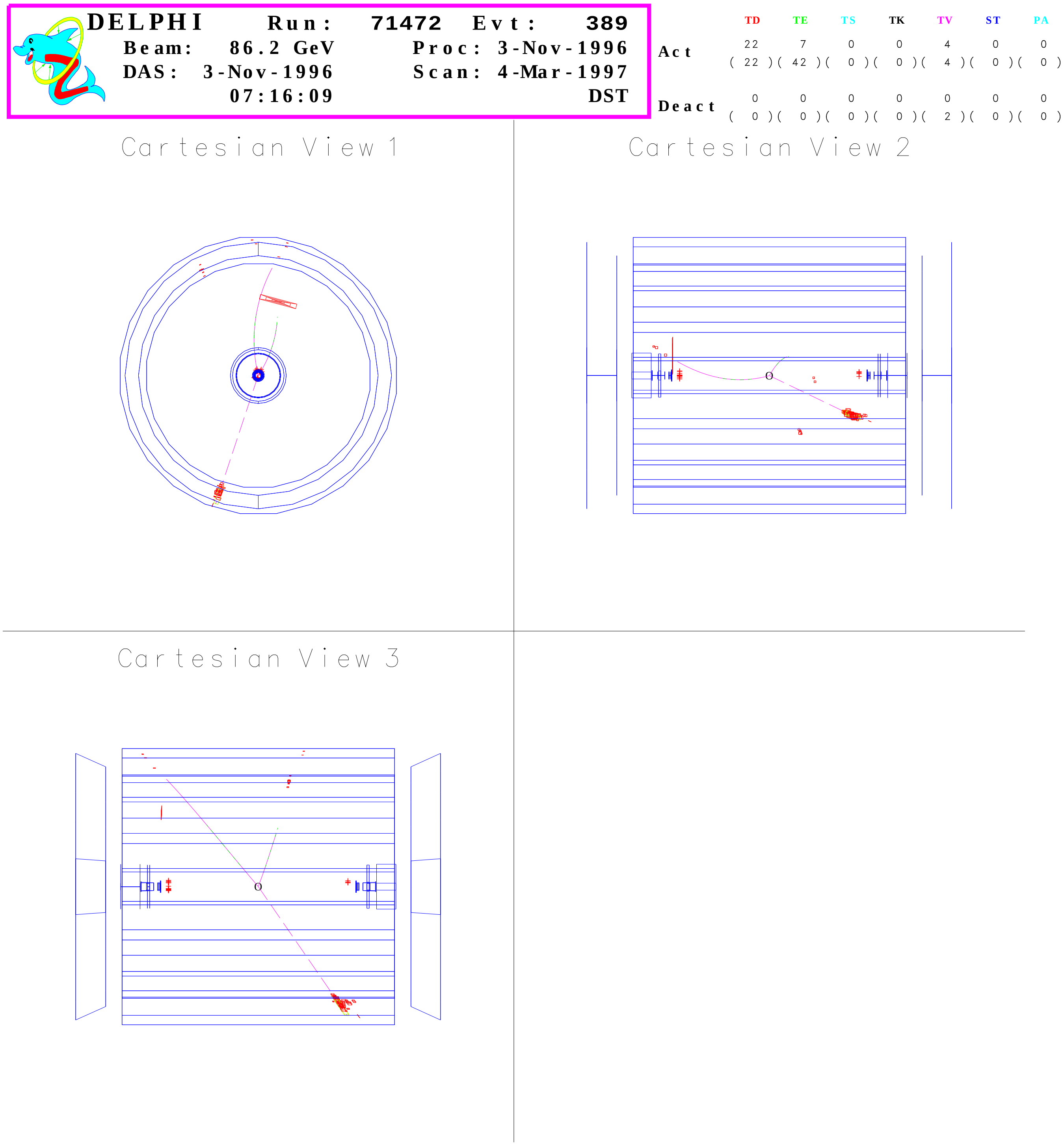

Figure 8: *The candidate selected in the search for charginos mass degenerate with the LSP. Not visible in the picture, there are 33.6 GeV deposited in one sector of the VSAT. The photon in the HPC has an energy of 7.9 GeV. The sum of all other visible energies in the event (excluding the VSAT) is 4.7 GeV.*

other effect of the low efficiency is that its relative error is not negligible when computing the number of expected signal events. Then, it is not possible to apply the usual procedure of comparing that number (which is supposed to be fixed) to the upper limit, at a given confidence level, of the mean value μ of the Poissonian distribution of the number of events seen in the data, given the number of candidates and the expected background [3].

Here the comparison proceeds as follows. Whenever there is no evidence of signal above the expected background, one compares data and theoretical expectations and sets an upper limit, at a given confidence level (CL) η so that

$$N_{\text{exp}} - N_{\text{up}} > 0 \tag{15}$$

in at least a fraction η of all possible cases. N_{up} is the number of signal events compatible with the data, distributed as the μ parameter (mean value) of a Poissonian, given the number of candidates observed and the expected background contamination. N_{exp} is the theoretical expectation for the signal searched for and, at any energy point, it is related to the theoretical cross section, the collected luminosity and the (selection plus trigger) efficiency by:

$$N_{\text{exp}} = \sigma \, \mathcal{L} \, \varepsilon \tag{16}$$

In the present search, the only relevant uncertainty in equation (16) comes from the selection efficiency. Such an efficiency is estimated starting from a sample, of size N, of MC generated events passed through the full simulation of the detector: if, out of them, k events survive the selection cuts, then the most likely value of the efficiency is given by

$$\varepsilon = \frac{k}{N} \tag{17}$$

The 'true' efficiency is the parameter p of the binomial distribution from which k events have been extracted out of a total sample of N. It is distributed as:

$$\mathcal{F}(p)\, dp = (N+1) \ cdot \begin{pmatrix} k \\ N \end{pmatrix} p^k (1-p)^{N-k}\, dp \tag{18}$$

To compute the exclusion limits at the CL η, a simple MC has been created. It generates many values of the difference in (15), according to the statistical distributions of the two terms, and then finds out which is the value exceeded by only a fraction η of the whole generated sample.

To combine more energy points (the same would hold if one wants to combine the results of more than one experiment), the distribution of N_{up} in equation (15) can be estimated according to the extension of the formula of [3] to the case of more than one channel reported in [18], while N_{exp} is given by

$$N_{\text{exp}} = \sum_{\text{i}} \sigma_{\text{i}} \, \mathcal{L}_{\text{i}} \, \varepsilon_{\text{i}} \tag{19}$$

where, in the MC, any efficiency is sampled independently at any centre-of-mass.

Inserting the last two equations in (15), as before the new physics scenario is excluded at the CL η whenever $N_{\text{exp}} - N_{\text{up}} > 0$ in at least a fraction η of all possible cases.

The whole procedure is explained, with more details, in [19].

6.2 Limits

The difference in (15) is reported in figure 9 at the 95% CL as a function of the chargino mass and for the three $\Delta(M)$ considered here. The upper part of the figure shows the scenario in which the chargino is higgsino-like, while below are the results for a gaugino like chargino. The different sensitivity of the two scenarios comes only from the production cross section, which is approximately three times larger in the second case. Since only chargino masses of 45, 50, 60 and 70 GeV$/c^2$ have been generated and passed through the full DELPHI simulation, the interpolation needed to find the point at which the difference crosses the value of 0 (which corresponds to the mass limit at that confidence level) has been performed by weighting the efficiencies calculated by the full simulation with the ones derived with a fast simulation at the generator level for intermediate masses and at all centre-of-mass energies.

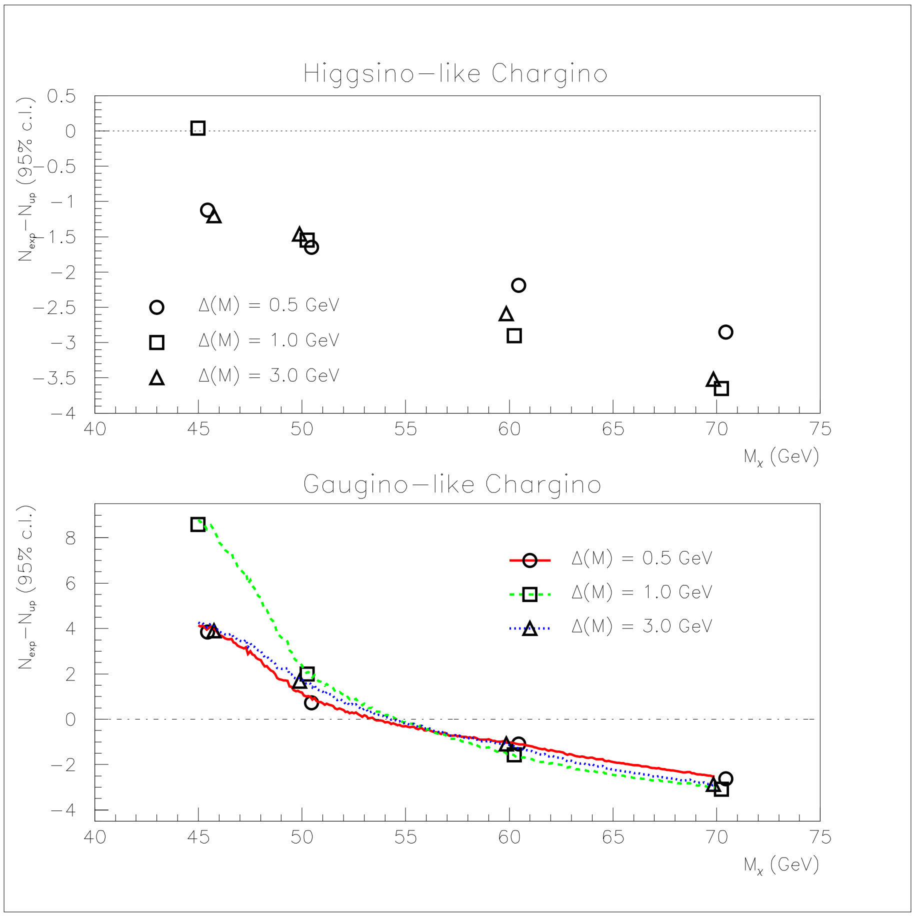

Figure 9: 95% *CL on the difference between the number of chargino events expected and the maximum number allowed in the data, as a function of the chargino mass. Whenever the difference is above* 0*, the point can be excluded at the same confidence level.*

The gaugino-like scenario can be excluded at the 95% CL for the lightest chargino having a mass below 53.4 GeV$/c^2$. For this limit, the most conservative between the three limits computed for $\Delta(M) = 0.5\,,1\,,3$ GeV has been taken. With the present statistics one cannot, however, improve the limit already obtained at LEP1 in the higgsino scenario; only for $\Delta(M) = 1$ GeV$/c^2$ charginos a lower limit on the mass can be set, which is 45.4

GeV/c^2 at the 95% CL and 48.2 GeV/c^2 at the 90% CL. As a comparison, at the 90% CL the gaugino-like scenario can be excluded up to chargino masses of 57.0 GeV/c^2, for all degeneracies between 0.5 and 3 GeV/c^2.

The limits obtained in the gaugino scenario at every mass difference considered, in the two cases of 95 and 90% CL, are detailed in table 5.

$\Delta(M)$ (GeV)	95% CL	90% CL
0.5	53.4 GeV	57.0 GeV
1	54.5 GeV	57.0 GeV
3	54.2 GeV	58.1 GeV

Table 5: 95% *and* 90% *confidence level upper limits on the mass of the gaugino-like chargino at the three degeneracies tested.*

All these results take into account a variation of $\tan\beta$ between 1 and 50; the mass of the sneutrino above $M(\tilde{\chi}_1^+)$ for the higgsino-like chargino and above 500 GeV/c^2 for the gaugino-like one; the M_2 and μ parameters chosen so that the mass difference between the chargino and the LSP remains inside the 0.5-3 GeV/c^2 interval.

7 Conclusions

A first attempt to look for sparticles mass-degenerate with the LSP has made using the data collected by the DELPHI experiment during all runs of LEP above the Z^0 pole energy. When using the initial state photon radiation tag, the otherwise overwhelming two photon background can be reduced to acceptable rates, although such a tag also strongly affects the efficiency of the signal searched for.

It is then necessary to combine all the statistics collected so far at the different LEP2 centre-of-mass energies to get appreciable sensitivity to the signal. No evidence of it has been found. The existence of charginos having a mass difference with the LSP between 0.5 and 3 GeV/c^2 can be excluded at the 95% confidence level for $M(\tilde{\chi}_1^+) < 53.4$ GeV/c^2, provided the chargino is gaugino-like.

Acknowledgements

We thank M. Drees for providing the program to compute the chargino branching ratios at low $\Delta(M)$; S. Katsanevas for explaining to us the features of SUSYGEN; V. Canale, C. Lacasta and G. Valenti for their support in analizing the data of the DELPHI trigger; J. Guy for his help in producing the full simulation of our special MC samples; F.L. Navarria for the stimulating discussions.

References

[1] H. P. Nilles, Phys. Rep. **110** (1984) 1;
H.E. Haber and G.L. Kane , Phys. Rep. **117** (1985) 75.

[2] P. Abreu et al. (DELPHI Coll.), Phys. Lett. **B382** (1996) 323;
P. Abreu et al. (DELPHI Coll.), Phys. Lett. **B387** (1996) 651.

[3] Particle Data Group J.J.Hernandez et al., Phys. Rev. **54D** (1996).

[4] P. Abreu et al. (DELPHI Coll.), CERN-PPE 96-188.

[5] C. Lacasta, DELPHI note in preparation.

[6] C.H. Chen, M. Drees, J.F. Gunion, Phys. Rev. Lett. **76** (1996) 2002.

[7] P. Aarnio, et al., (DELPHI coll.), Nucl. Inst. Meth. **A303** (1991) 233;
P. Abreu, et al, (DELPHI coll.), Nucl. Inst. Meth. **A378** (1996) 57.

[8] T. Sjöstrand, Comp. Phys. Comm. **39** (1986) 347;
T. Sjöstrand, "PYTHIA 5.6 and JETSET 7.3", CERN-TH/6488/92.

[9] DELSIM users guide and reference manual, DELPHI note 89-15 PROG 130 and 89-69 PROG 143.

[10] S. Katsanevas and S. Melanchroinos in "Physics at LEP2", CERN 96-01 (Vol.2) 328.

[11] F.A. Berends, P.H. Daverveldt, R. Kleiss, Nucl. Phys. **B253** (1985) 421;
Comp. Phys. Comm. **40** (1986) 271, 285 and 309.

[12] S. Nova, A. Olshevskyi, T. Todorov, DELPHI note 90-35 (1995).

[13] C.H. Chen, M. Drees, J.F. Gunion, Phys. Rev. **D76** (1997) 330.

[14] M. Feindt, C. Kreuter, O. Podobrin, DELPHI 96-82 PROG 217.

[15] A.C. Benvenuti, et al., IEEE Trans. Nucl. Sci. **40** (1993) 537.

[16] V. Bocci, et al., Nucl. Inst. Meth. **A362** (1995) 361;
V. Canale, G. Valenti, DELPHI 96-104 DAS 179.

[17] P. Abreu, et al. (DELPHI coll.) CERN-PPE/96-03 (revised), to appear in Z. Phys. C;
W. Adam, et al. (DELPHI coll.), Phys. Lett. **B380** (1996) 471.

[18] V.F.Obraztsov, Nucl. Inst. Meth. **A316** (1992) 388.

[19] A. Perrotta, DELPHI note in preparation.